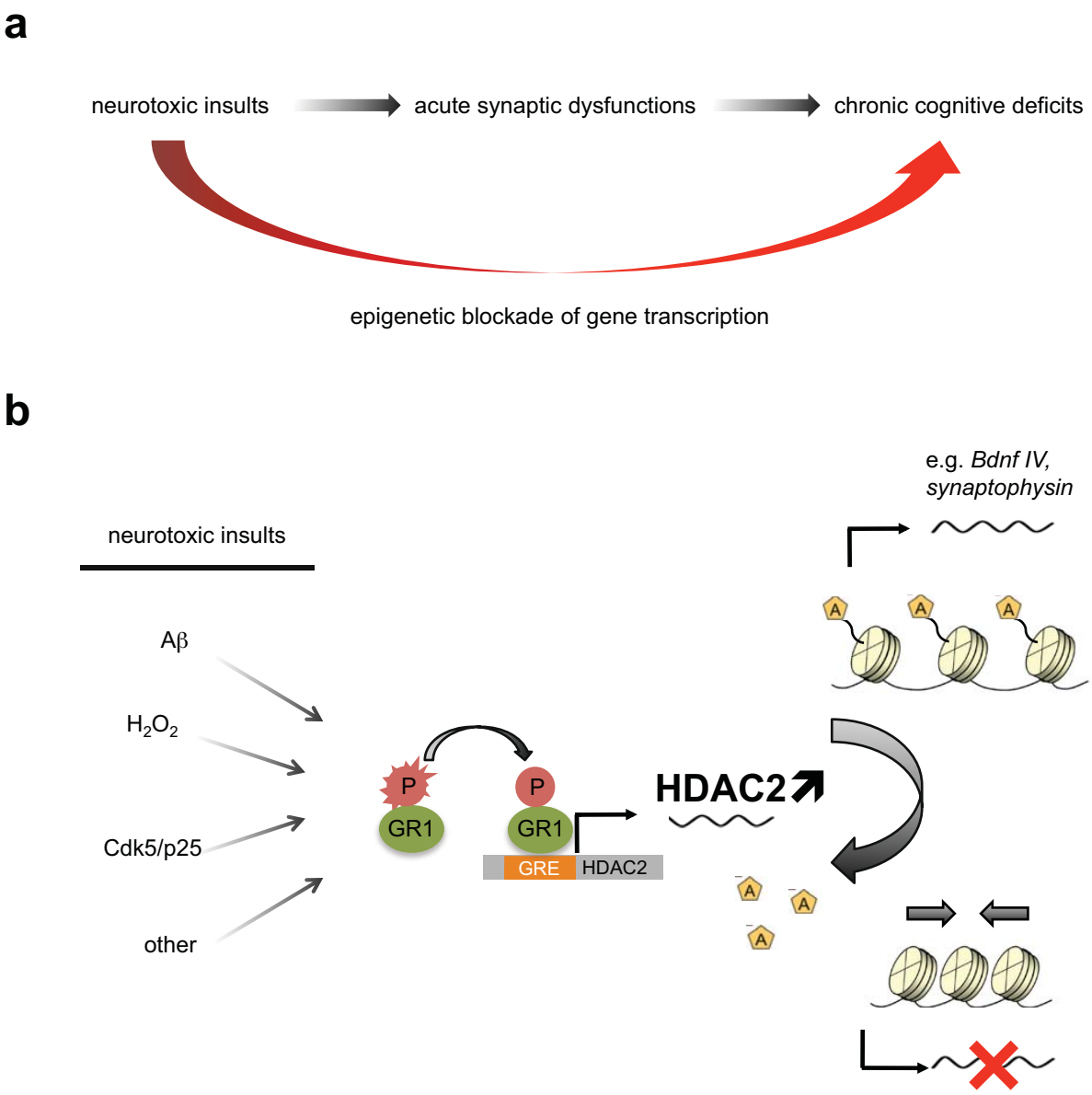

Supplementary Figure 1. Model of the potential consequences and causes of elevated HDAC2 levels in the neurodegenerating brain. a, Neurotoxic insults are known to acutely constrain synaptic functions, which in turn, can lead to more chronic cognitive dysfunctions. Here, we propose that neurotoxic insults can directly lead to cognitive dysfunctions by epigenetically silencing neuroplasticity genes via the mechanisms described below. **b**, Upon neurotoxic insults such as extracellular Aβ-fibrils, H_2O_2, intracellular accumulation of p25 and/or other stimuli, GR1 becomes phosphorylated on S211, a mark for its activation. Phoshorylated GR1 binds to its responsive element (GR responsive element, GRE) in the proximal HDAC2 promoter region in the neurodegenerating mouse brain, and stimulates the expression of *Hdac2*. In the presence of Aβ-fibrils and H_2O_2, this stimulation is further potentiated, but abolished when S211 is mutated to A211. Elevated HDAC2 protein levels bind to the promoter region of learning, memory and synaptic plasticity-related genes such as *BdnfIV*, *synaptophysin* and others. There, HDAC2 binding co-occurs with reduced histone acetylation, and thus more compacted chromatin, preventing RNA polymerase from binding, supposedly the driving force behind the reduced gene expression observed. Such decreased expression of neuroplasticity genes is correlated with reduced synaptic plasticity and poor memory performance in mice with neurodegeneration.

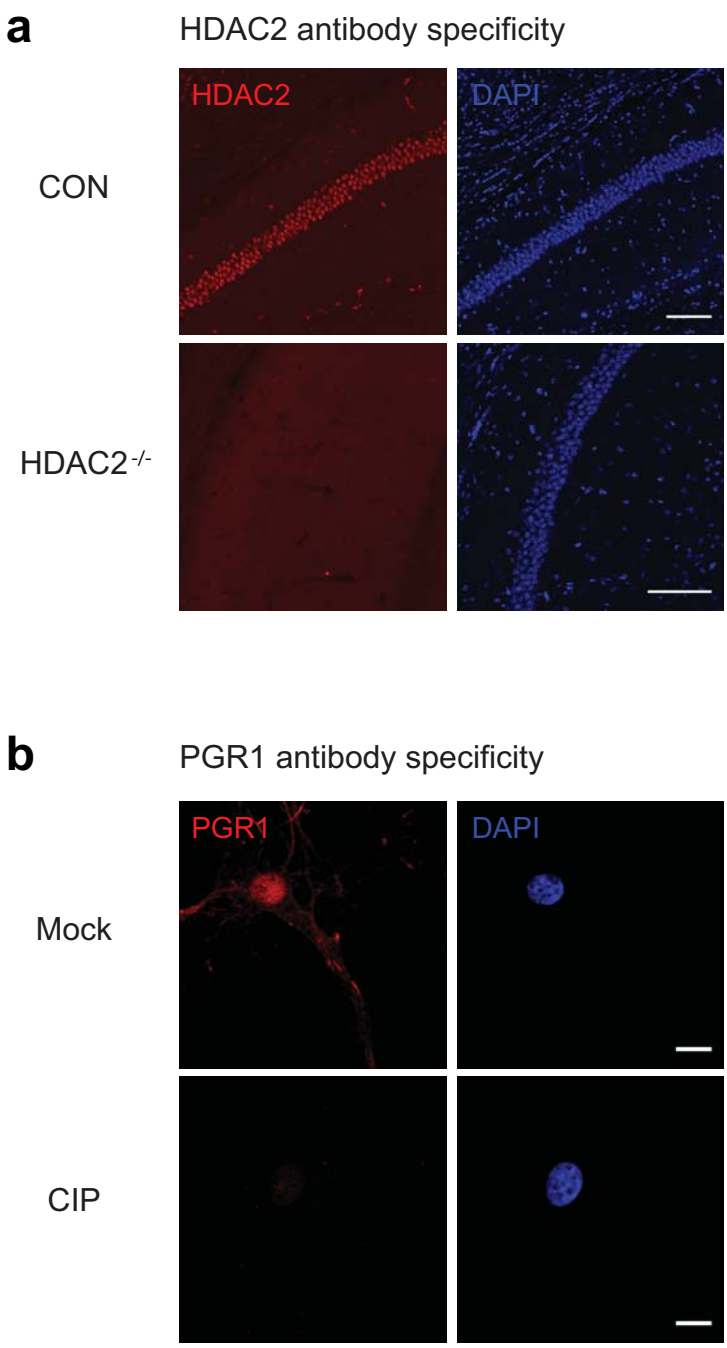

Supplementary Figure 2. Specificity of HDAC2 and PGR1 antibody signals. a, Immunohistochemical images showing HDAC2 detection in the hippocampus of wild-type mice, but not in HDAC2-/- mice. Scale bar upper panel, 80µm, lower panel, 100µm. **b**, Immunocytochemical images showing PGR1 immunoreactivity in mock-treated, but not in calf intestinal phosphatase (CIP)-treated primary hippocampal neurons (DIV14). Scale bar, 10µm.

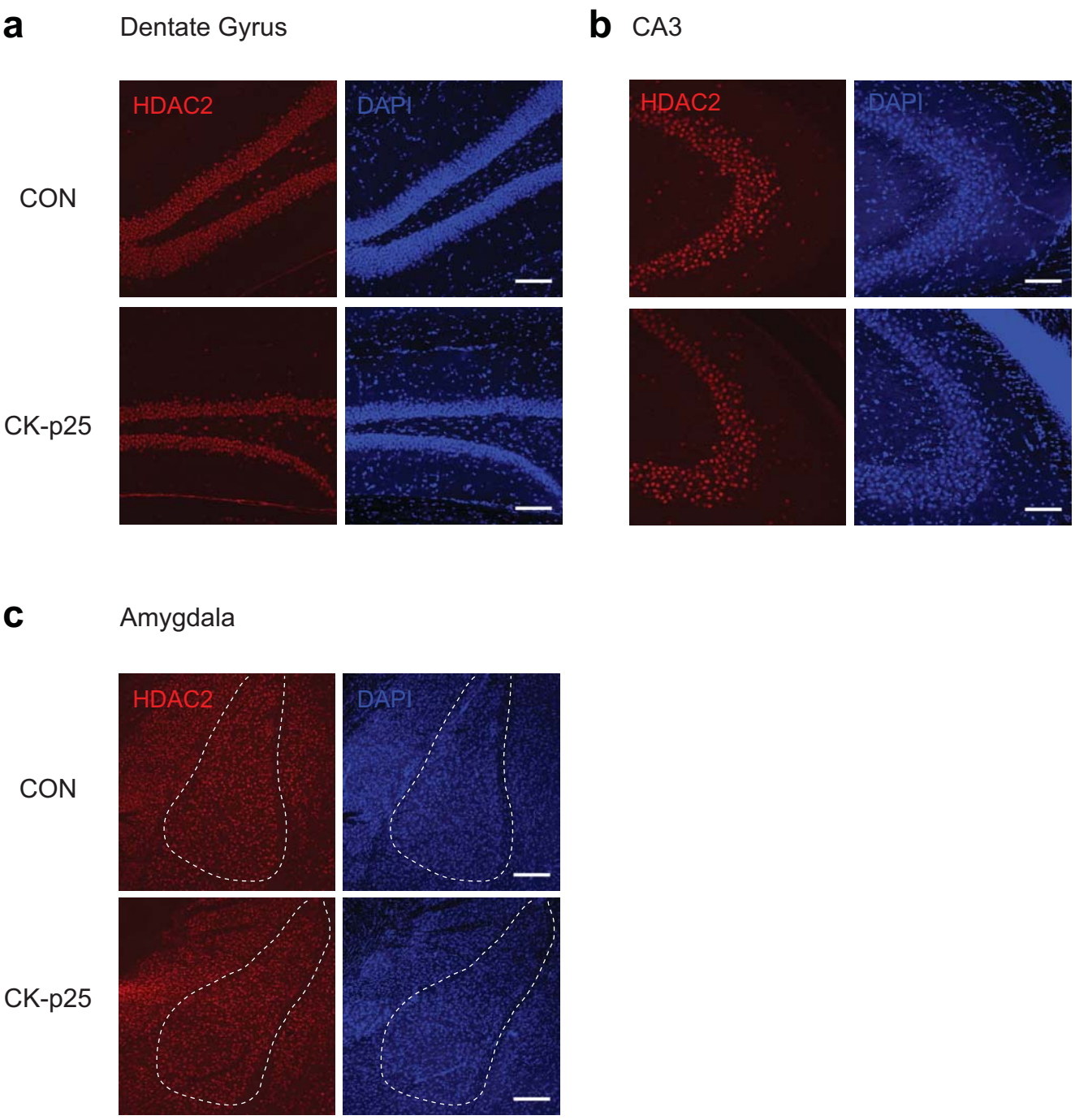

Supplementary Figure 3. The elevation of HDAC2 is restricted to area CA1 of the hippocampus, and further not observed in the amygdala. a, **b**, Representative immunohistochemical images of HDAC2 levels in the (**a**) dentate gyrus and (**b**) hippocampal area CA3 of CK-p25 mice compared to control littermates. **c**, Representative immunohistochemical images of HDAC2 levels in the amygdala of CK-p25 mice compared to control littermates; scale bar, 100μm (**a**, **b**), 200μm (**c**).

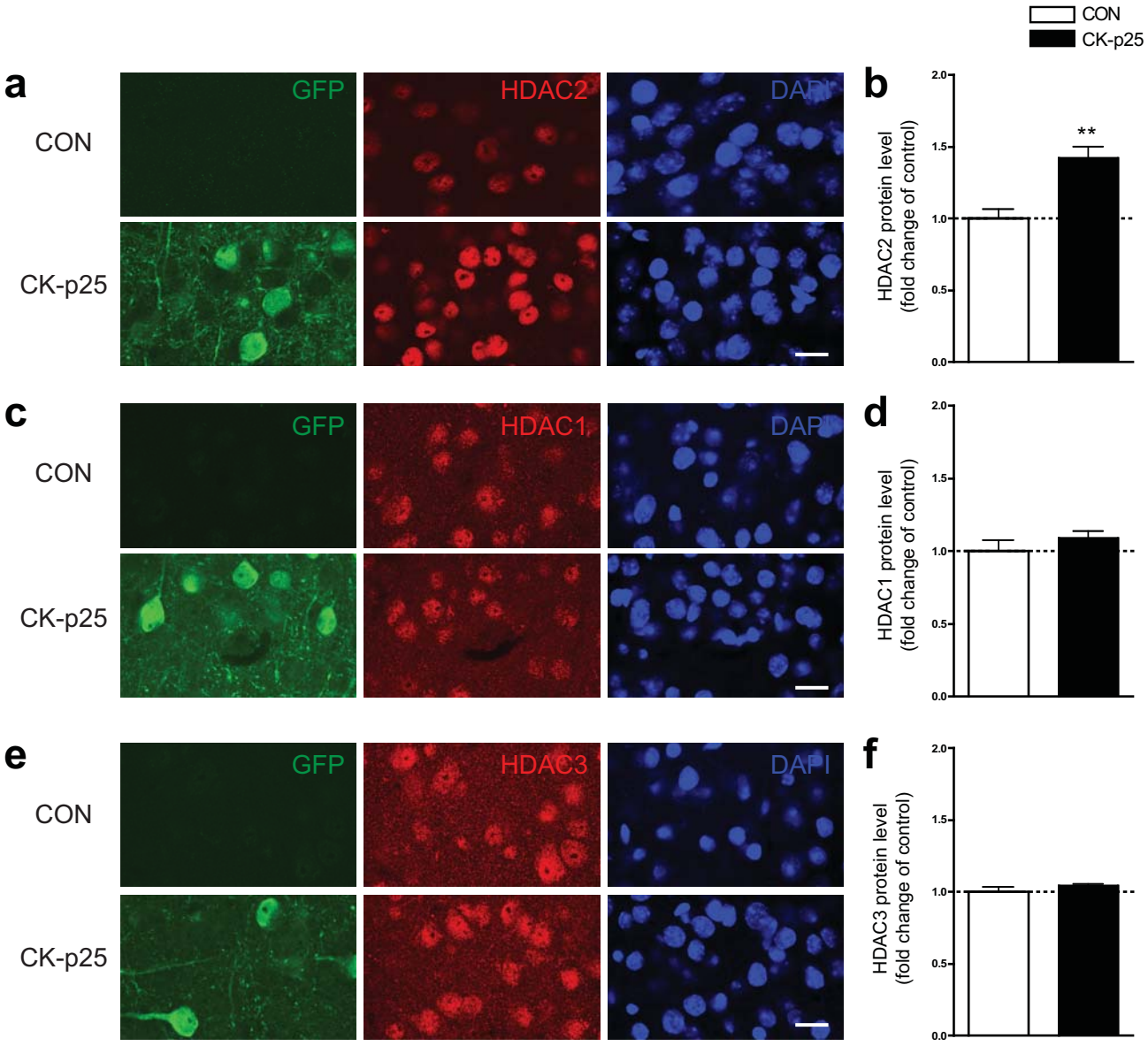

Supplementary Figure 4. HDAC2, but not HDAC1 and HDAC3, is increased in the neurodegenerating cortex of CK-p25 mice. a-c, Representative immunohistochemical images depicting (**a**) HDAC2, (**b**) HDAC1, and (**c**) HDAC3 levels in the prefrontal cortex of CK-p25 mice and control littermates (n=3-6 sections from 3 mice each). **d-f**, Quantification of (**a-c**). Scale bar, 20μm. **p≤0.01; values are mean ± s.e.m.

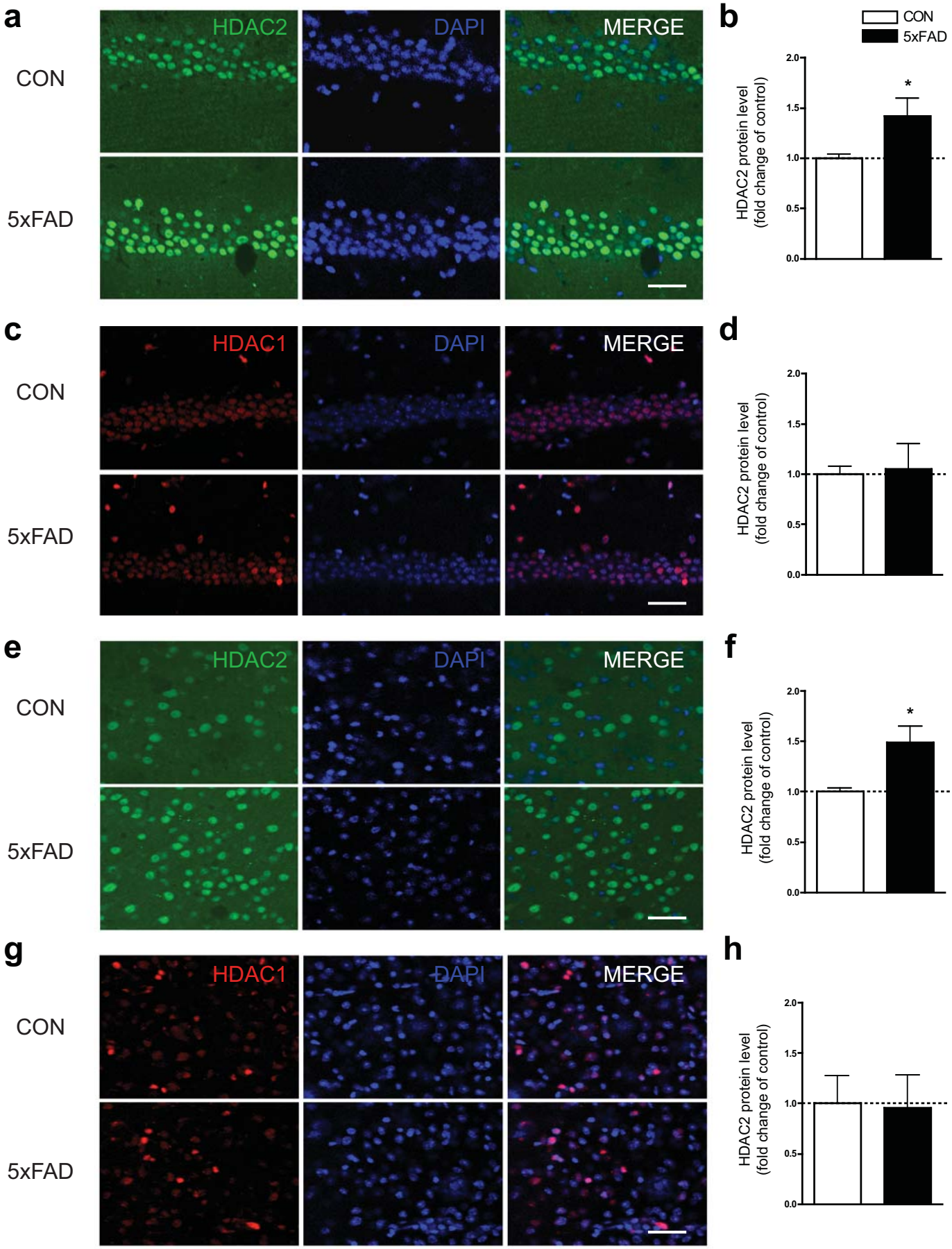

Supplementary Figure 5. HDAC2, but not HDAC1 levels are increased in the neurodegenerating forebrain of 5xFAD mice. a, **c**, Representative immunohistochemical images depicting (**a**) HDAC2 and (**c**) HDAC1 in the hippocampus of 6-month old 5xFAD mice compared to control littermates (n=3-6 sections from 3-4 mice each). **b**, **d**, Quantitative assessment of (**a**) and (**c**). **e**, **g**, Representative immunohistochemical images depicting (**e**) HDAC2 and (**g**) HDAC1 in the prefrontal cortex of 6-month old 5xFAD mice compared to control littermates (n=3-4 sections from 3 mice each). **f**, **h**, Quantitative assessment of (**e**) and (**g**). Scale bar, 50μm. *p≤0.05; values are mean ± s.e.m.

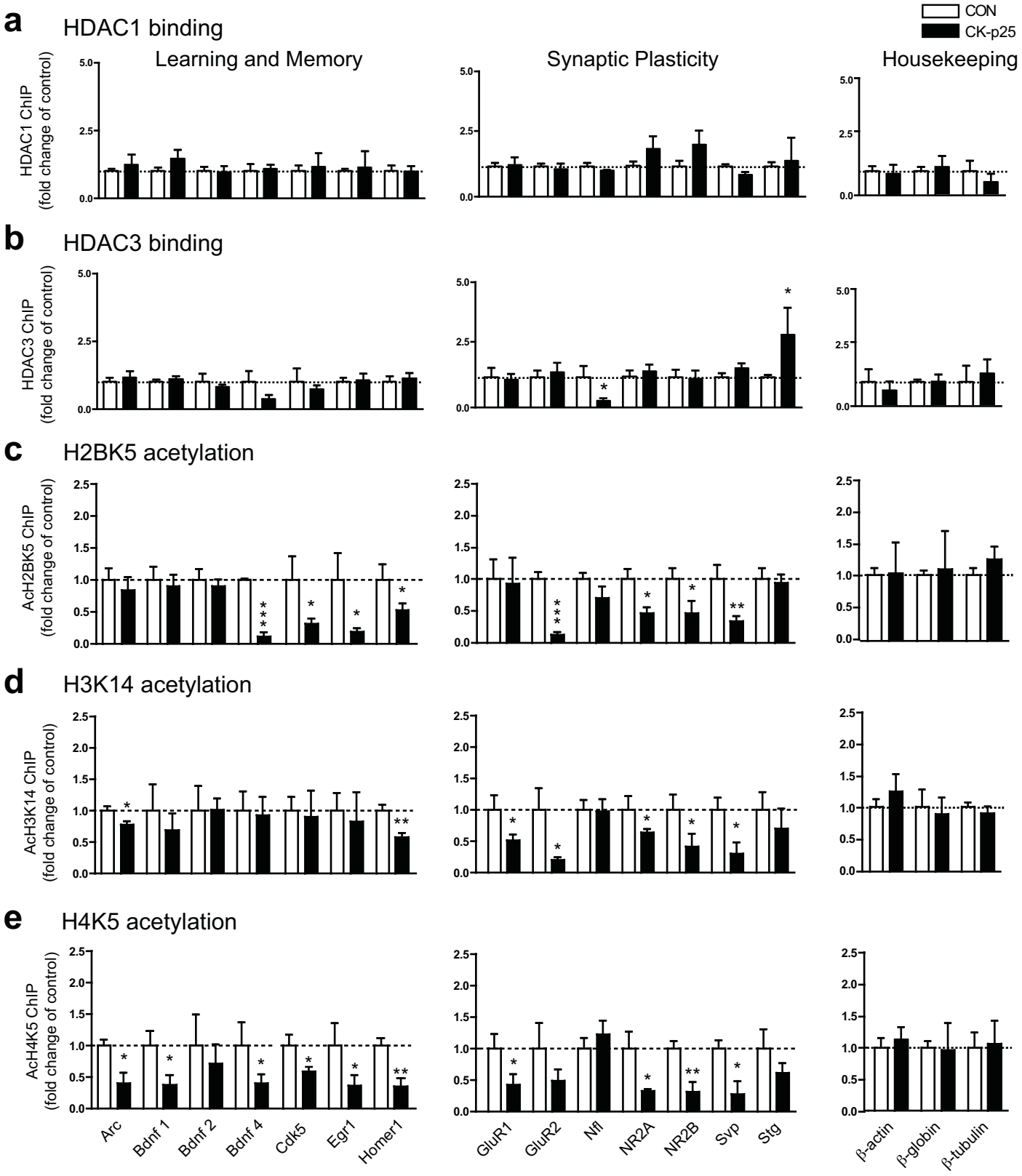

Supplementary Figure 6. HDAC1 and HDAC3 binding to neuroplasticity genes is overall not increased in the hippocampus of CK-p25 mice, but the reduction of histone acetylation in the promoter region of neuroplasticity genes is not restricted to H4K12. a, **b**, Quantitative PCR results of (**a**) HDAC1- and (**b**) HDAC3-immunoprecipitated chromatin in the hippocampus of CK-p25 mice versus control littermates (n=4-6 mice each). **c**-**e**, Quantitative PCR results of (**c**) AcH2BK5-, (**d**) AcH3K14- and (**e**) AcH4K5-immunoprecipitated chromatin of the hippocampus of CK-p25 mice versus control littermates (n=3-8 animals each). *p≤0.05; **p≤0.01; ***p≤0.001; values are mean ± s.e.m.

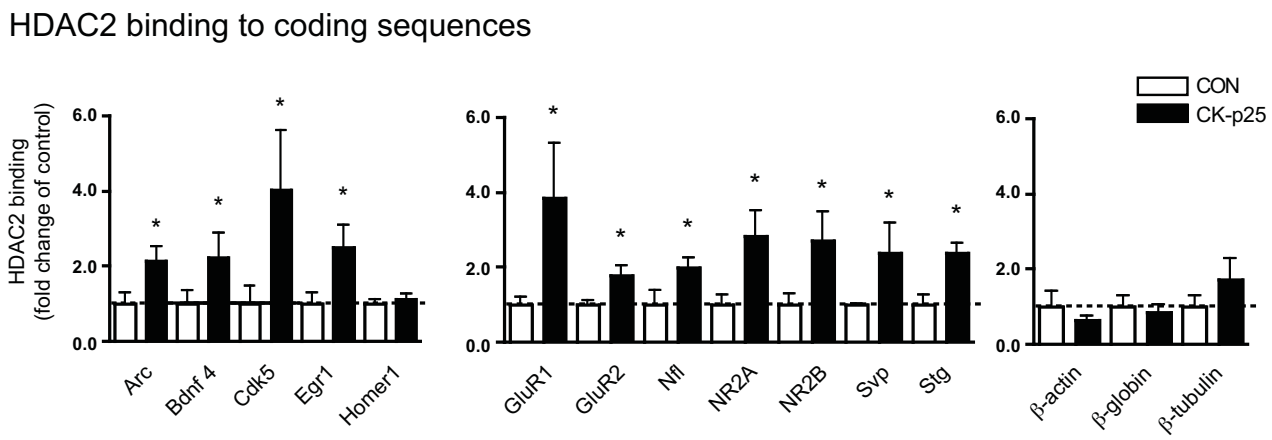

Supplementary Figure 7. HDAC2 binding to the coding region of neuroplasticity genes is increased in the hippocampus of CK-p25 mice. Quantitative PCR results of HDAC2-immunoprecipitated chromatin in the coding sequence of neuroplasticity genes in the hippocampus of CK-p25 mice versus control littermates (n=4-5 animals each). *p≤0.05; values are mean ± s.e.m.

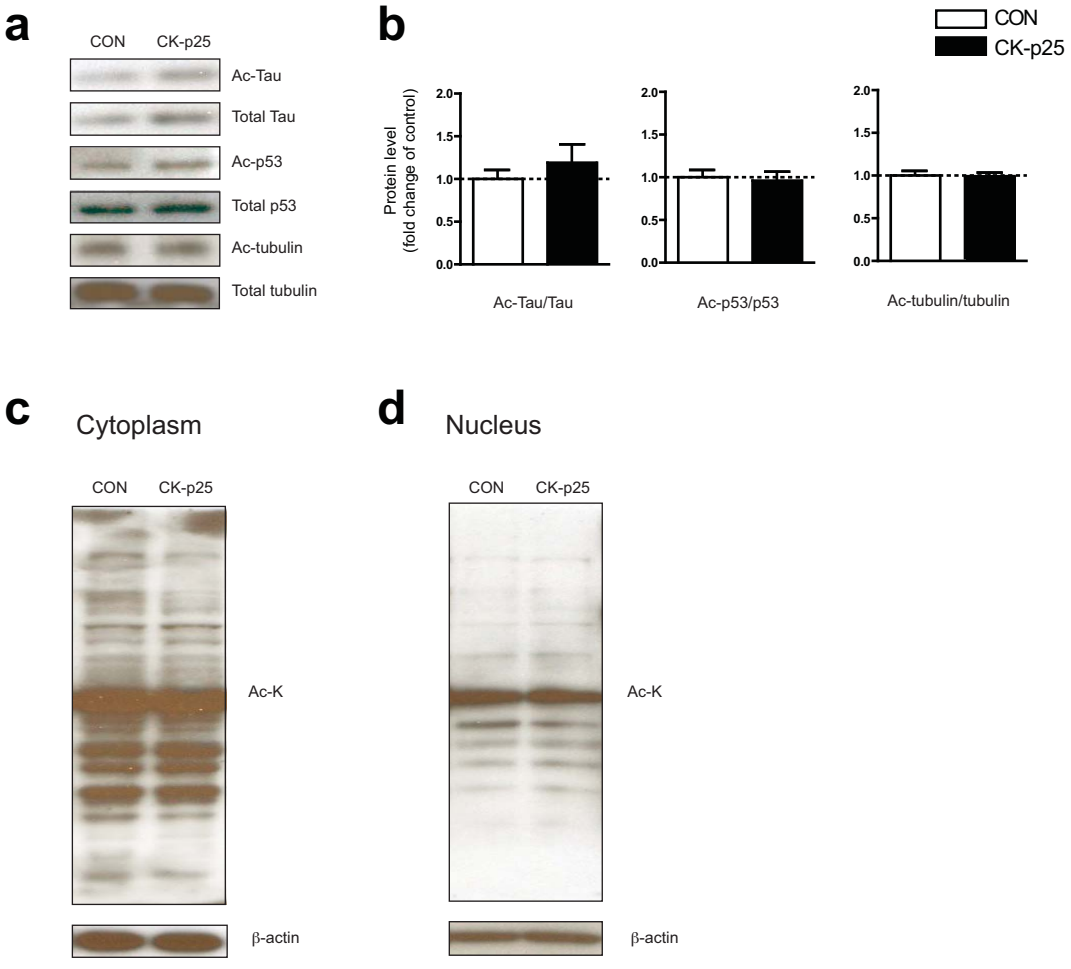

Supplementary Figure 8. The elevation of HDAC2 does not induce overt acetylation changes on proteins other than histones. a, Representative images of acetyl western blot analysis of immuno-precipitated protein complexes with tau, p53 and tubulin (n=3-6 mice each); note that the increase in tau and p53 protein levels in the CK-p25 mice has been previously described. **b**, Quantification of (**a**). **c**, **d**, Representative images of western blot analysis of protein acetylation in cytoplasmic (**c**) and nuclear (**d**) hippocampal extracts of CK-p25 mice and control littermates (n=3 mice each); values are mean ± s.e.m.

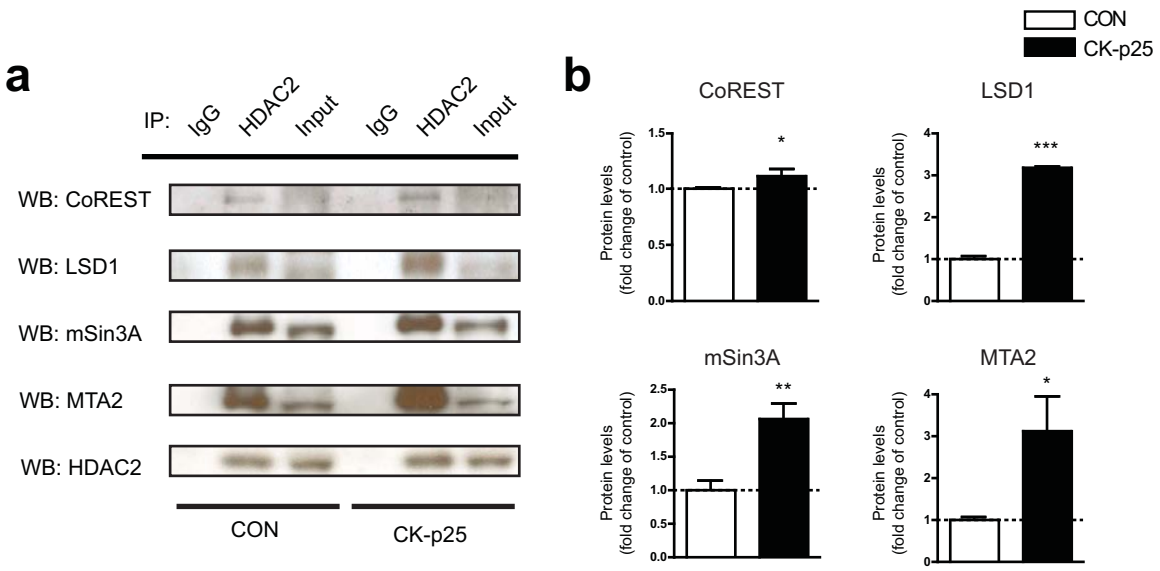

Supplementary Figure 9. HDAC2 is more abundantly bound to co-repressor complexes in the hippocampus of CK-p25 mice. a, Representative images of western blot analysis of protein levels of CoREST and LSD1, members of the CoREST complex, of mSIN3A, a member of the Sin3 complex, and of MTA2, a member of the NuRD complex, following immunoprecipitation of hippocampal extracts with HDAC2 (n=3-4 animals each for CK-p25 and control groups). **b**, Quantification of (**a**). Protein levels were normalized to input, *p≤0.05; **p≤0.01; ***p≤0.001; values are mean ± s.e.m.

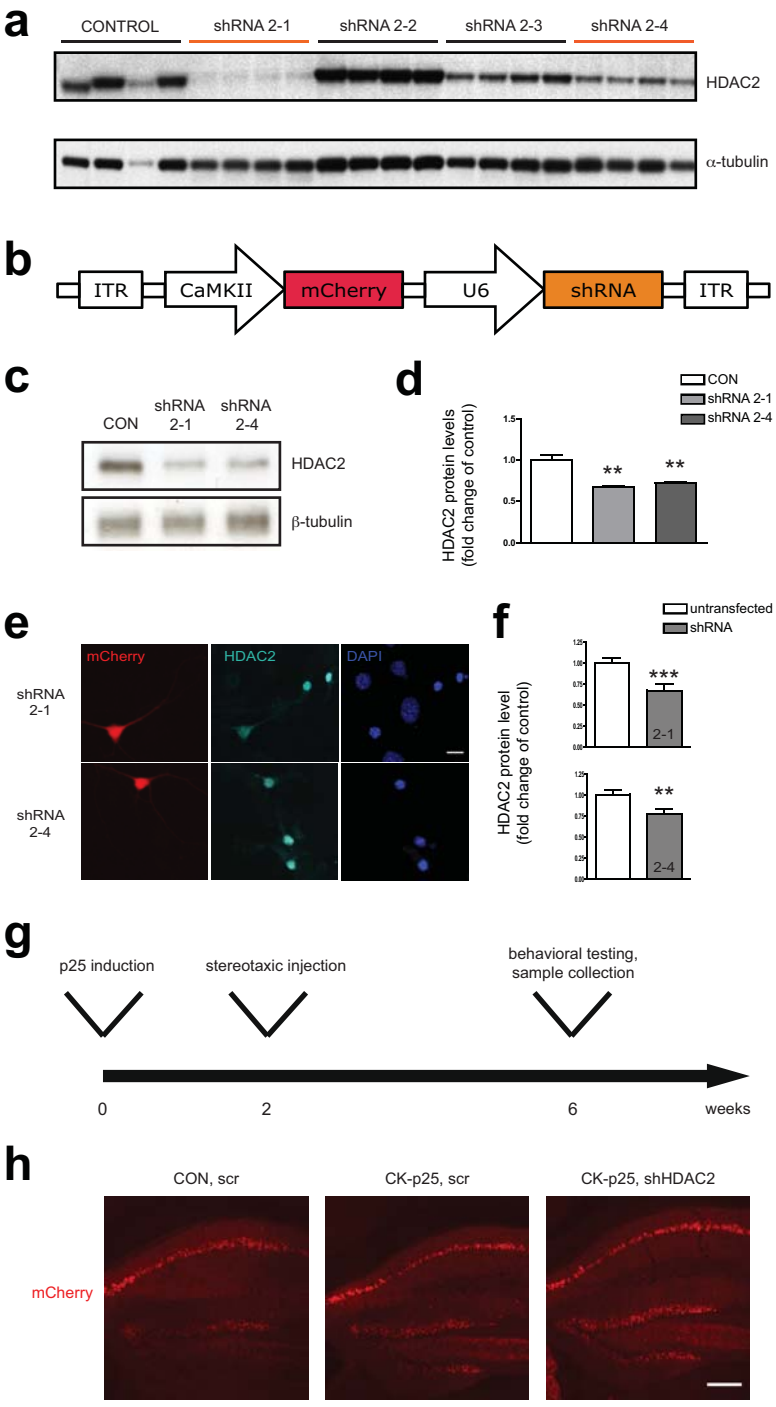

Supplementary Figure 10. Strategy to reduce HDAC2 expression by RNA interference. a, Validation of the target specificity of different HDAC2 shRNA clones as determined by lentiviral transduction in primary cortical neurons by western blot analysis. A significant downregulation was observed for constructs shRNA2-1 and shRNA2-4. These constructs and the scramble shRNA were then subcloned into the AAV vector under (**b**). **b**, Schematic of the construct used for AAV production; "shRNA" signifies either control scramble shRNA, or shRNA constructs targeting HDAC2. **c**, Representative images of western blot analysis of HDAC2 in primary hippocampal neurons (DIV14) following transfection with the AAV-shRNA constructs. **d**, Quantification of (**c**). **e**, Representative immunocytochemical images depicting HDAC2 levels in primary hippocampal neurons (DIV14) following transfection with the AAV-shRNA constructs; scale bar, 1μm. **f**, Quantification of (**e**). **g**, Schematic of the experimental timeline. Mice were 3-4 months of age when p25 was induced, and the viruses injected 2 weeks later. **h**, Representative pictures of mCherry showing comparable infection rates in hippocampal area CA1 of control mice injected with scrambled shRNA (CON, scr), CK-p25 mice injected with scrambled shRNA (CK-p25, scr) and CK-p25 mice injected with the shRNA against HDAC2 (CK-p25, shHDAC2); scale bar, 100μm. **p≤0.01; ***p≤0.001; values are mean ± s.e.m.

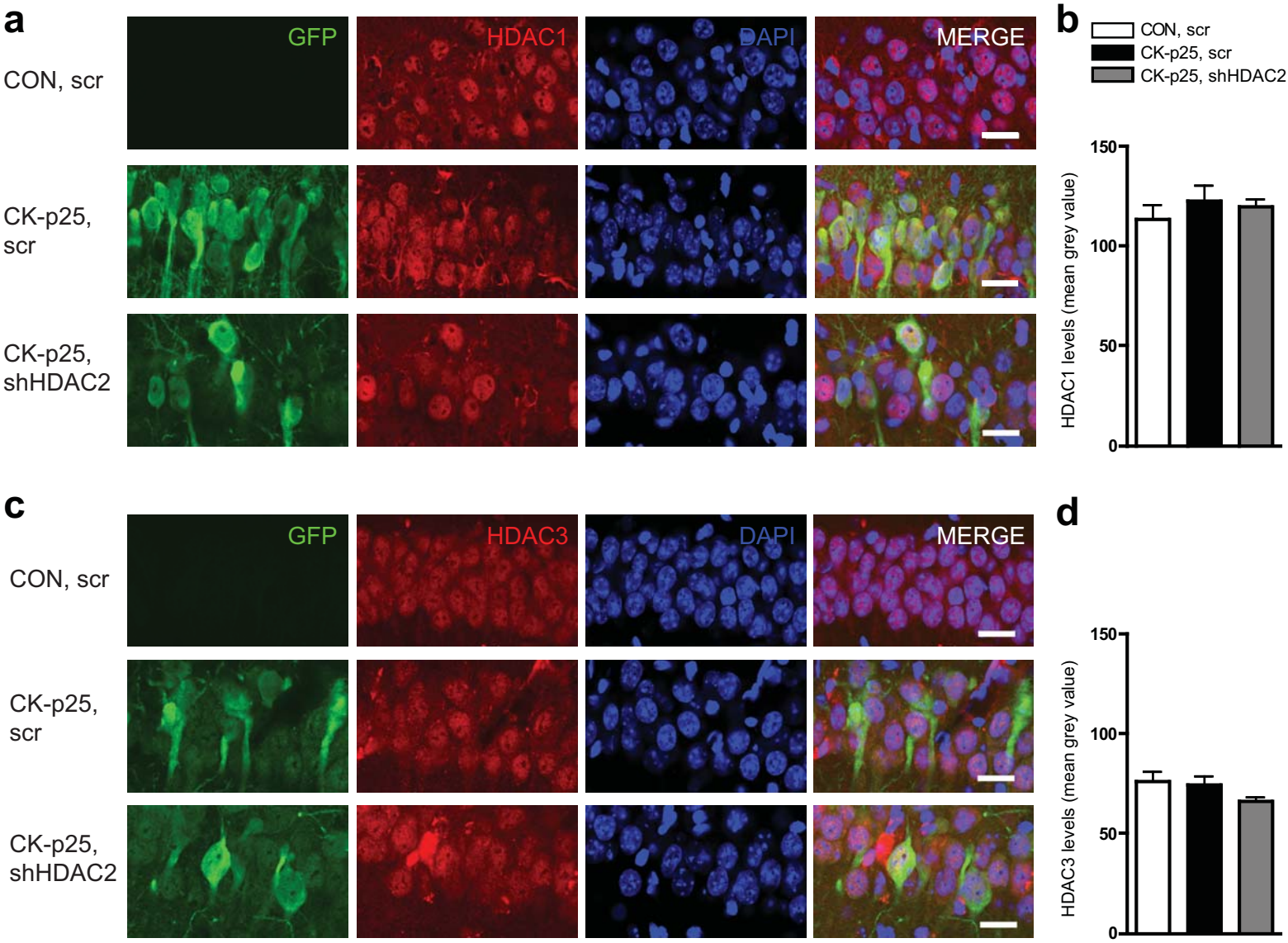

Supplementary Figure 11. AAV-shRNA mediated knockdown of HDAC2 does not alter levels of HDAC1 and HDAC3. **a**, **c**, Representative immunohistochemical images depicting hippocampal (**a**) HDAC1 and (**c**) HDAC3 levels in CON, scr, CK-p25, scr, and CK-p25, shHDAC2 animals (n=4-5 sections from 4 mice each). **b**, **d**, Quantitative assessment of (**a**, **c**); scale bar, 20μm; values are mean ± s.e.m.

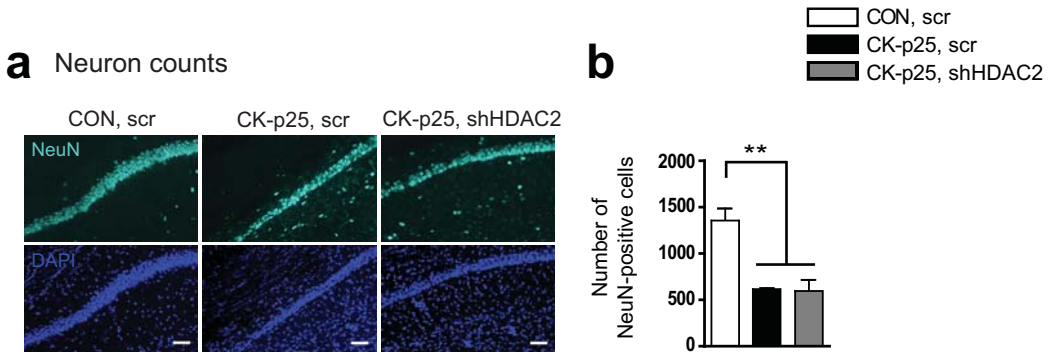

Supplementary Figure 12. Knock-down of HDAC2 does not alter the course of neurodegeneration. a, Representative immunohistochemical images depicting NeuN staining in hippocampal area CA1 of CON, scr, CK-p25, scr, and CK-p25, shHDAC2 animals (n=4-5 sections from 3-4 mice each). **b**, Quantification thereof; scale bar, 80µm; **p≤0.01; values are mean ± s.e.m.

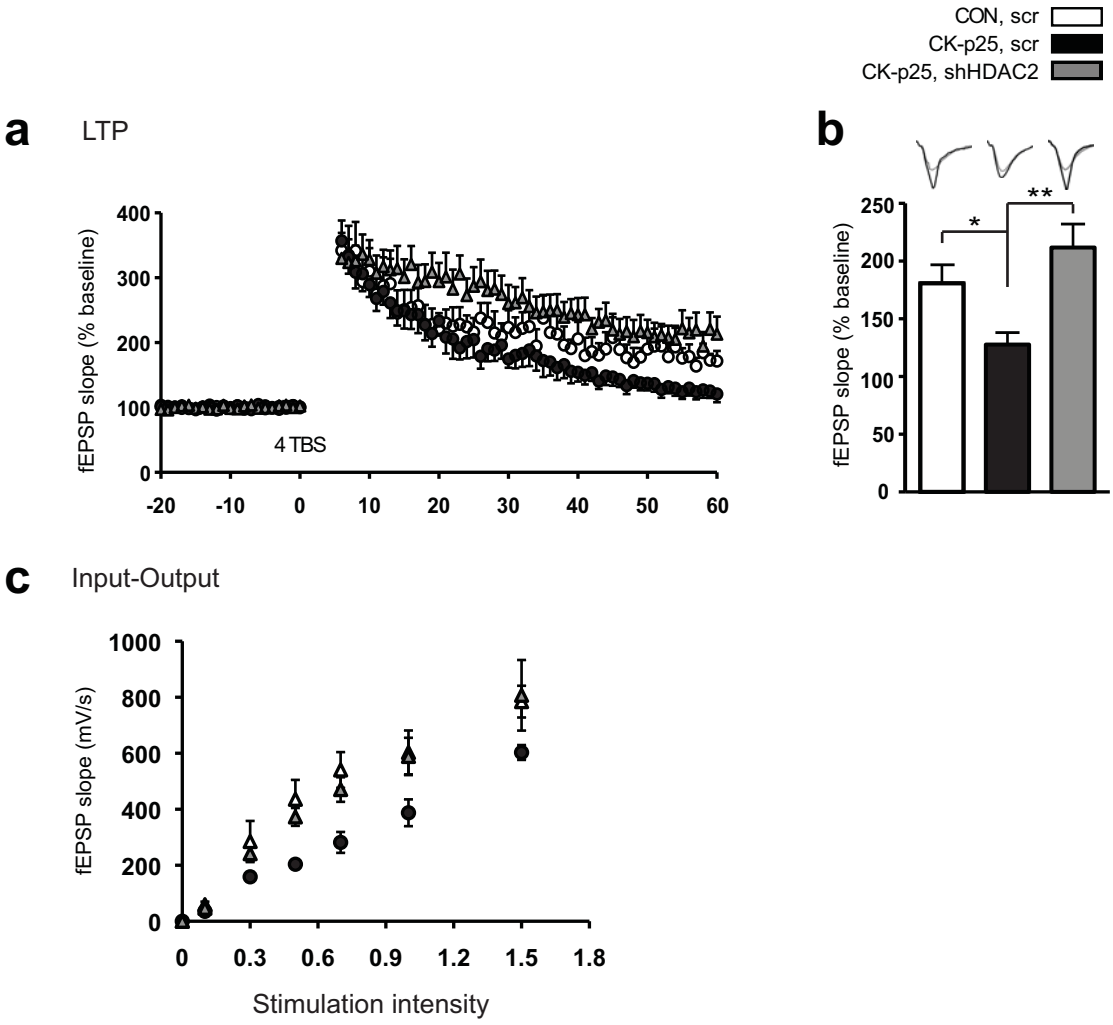

Supplementary Figure 13. Synaptic plasticity is restored upon reducing HDAC2. a, Field excitatory postsynaptic potential (fEPSP) slopes in the hippocampus CA1 of CON, scr, CK-p25, scr and CK-p25, shHDAC2 animals (n=7-8 slices from 4 mice each). **b**, Average slopes of fEPSP during the last 10min of recording; sample traces above the bar chart represent fEPSPs at 1min before (gray) and 1h after (black) theta-burst stimulation (TBS). **c**, Input/output relationship of baseline synaptic transmission. *p≤0.05; **p≤0.01; values are mean ± s.e.m.

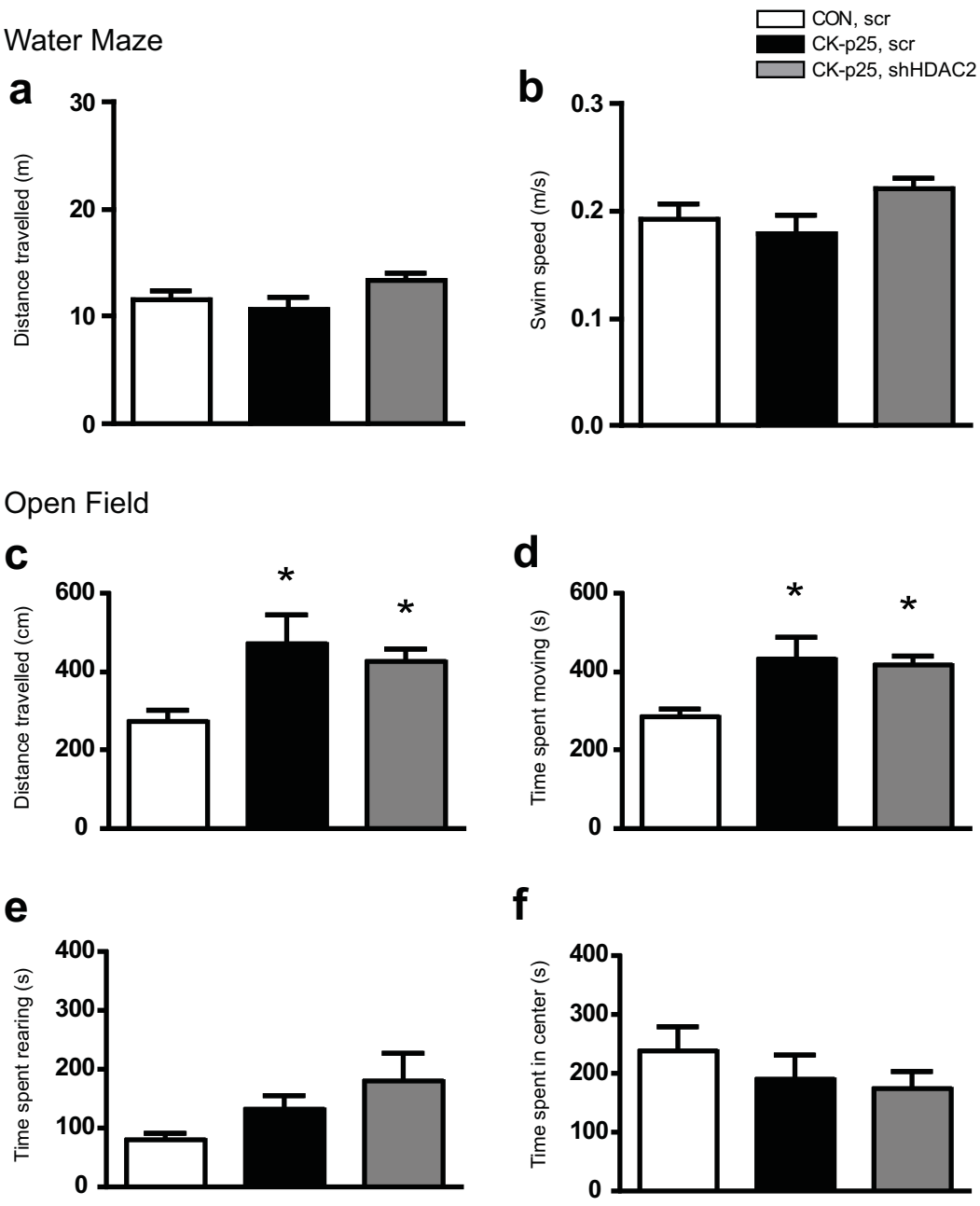

Supplementary Figure 14. Overall locomotion and anxiety behavior is not affected by AAV-mediated HDAC2 reduction. **a**, **b**, Distance travelled (**a**) and swim speed (**b**) were comparable between CON, scr, CK-p25, scr and CK-p25, shHDAC2 in the water maze task. **c**, **d**, Distance travelled (**c**) and time spent moving (**d**) were comparable between CK-p25, scr and CK-p25, shHDAC2 on an open field test. Note that both groups of CK-p25 animals were hyperactive as compared to CON, scr animals. **e**, **f**, Time spent rearing (**e**) and time spent in center (**f**) were comparable between CON, scr, CK-p25, scr, and CK-p25, shHDAC2 mice during an open field test. *p≤0.05; values are mean ± s.e.m.

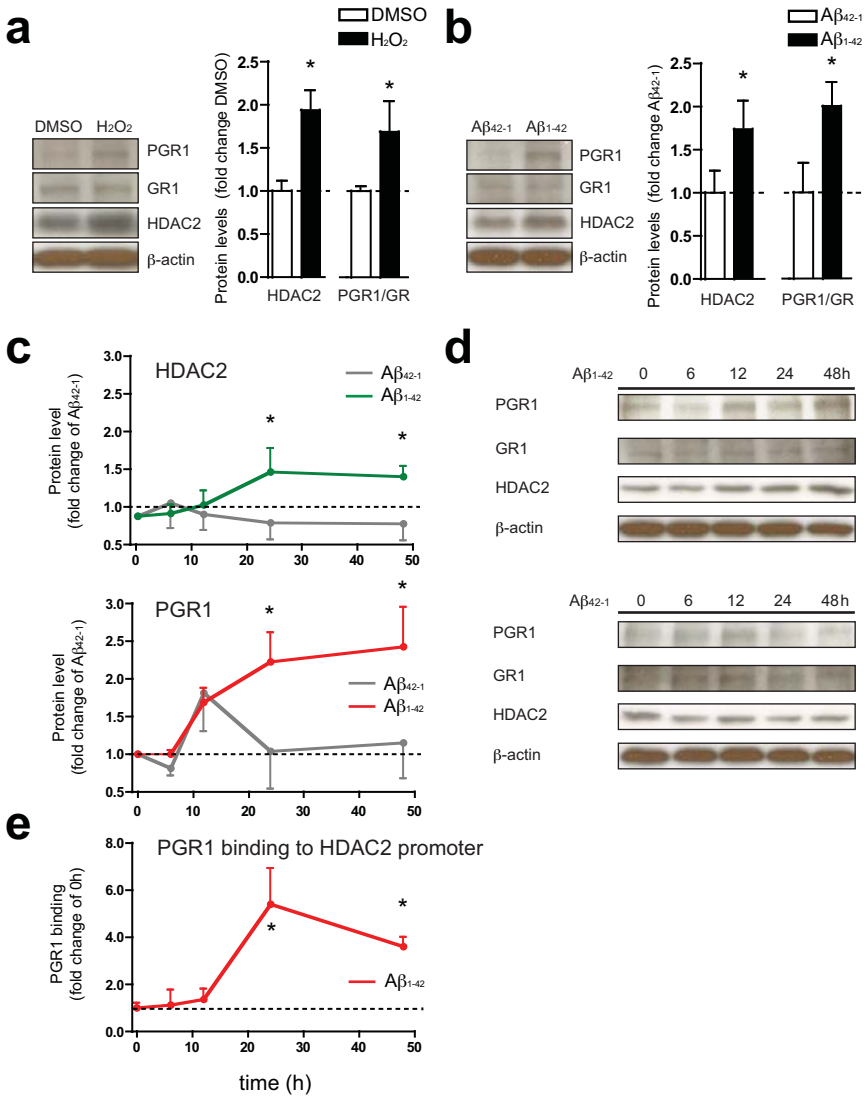

Supplementary Figure 15. Timecourse of PGR1 and HDAC2 induction following neurotoxic insults. a, **b**, Representative images (left) of western blot analyses of PGR1, GR1, and HDAC2 levels of primary hippocampal neurons after (**a**) H_2O_2-treatment and after (**b**) exposure to Aβ1-42 or Aβ42-1 oligomers and quantification thereof (right). PGR1 was normalized to GR1. **c**, **d**, Quantification (**c**) and representative images (**d**) of western blot analysis of PGR1 and HDAC2 induction in primary hippocampal neurons (DIV14) treated with Aβ1-42 or Aβ42-1 oligomers. PGR1 was normalized to GR1. **e**, Timecourse of PGR1 binding to the GRE in the HDAC2 promoter as revealed by ChIP analysis in primary cortical neurons (DIV10-14) treated with Aβ1-42. *p≤0.05; values are mean ± s.e.m.

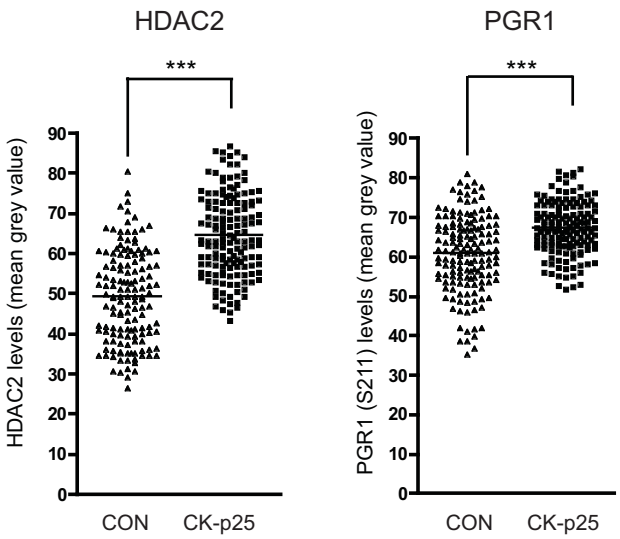

Supplementary Figure 16. HDAC2 and PGR1 protein levels are concomitantly increased in CK-p25 mice. Scatter plot representation of HDAC2 and PGR1 immunohistochemical labeling of hippocampal neurons in CK-p25 versus control mice (n=3-6 slices from 3 mice each); ***p≤0.001.

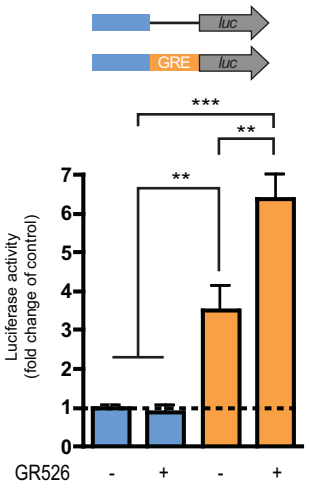

Supplementary Figure 17. GR526 potentiates the transcriptional potential of the GRE in the HDAC2 promoter. Luciferase activity of CAD cells (≥3 independent experiments) transfected with the proximal promoter region of HDAC2 with (orange) or without (blue) GRE (schematic of constructs are shown above the graph) and co-transfected with a constitutively active form of GR, GR526 (see Methods). **p≤0.01; ***p≤0.001; values are mean ± s.e.m.

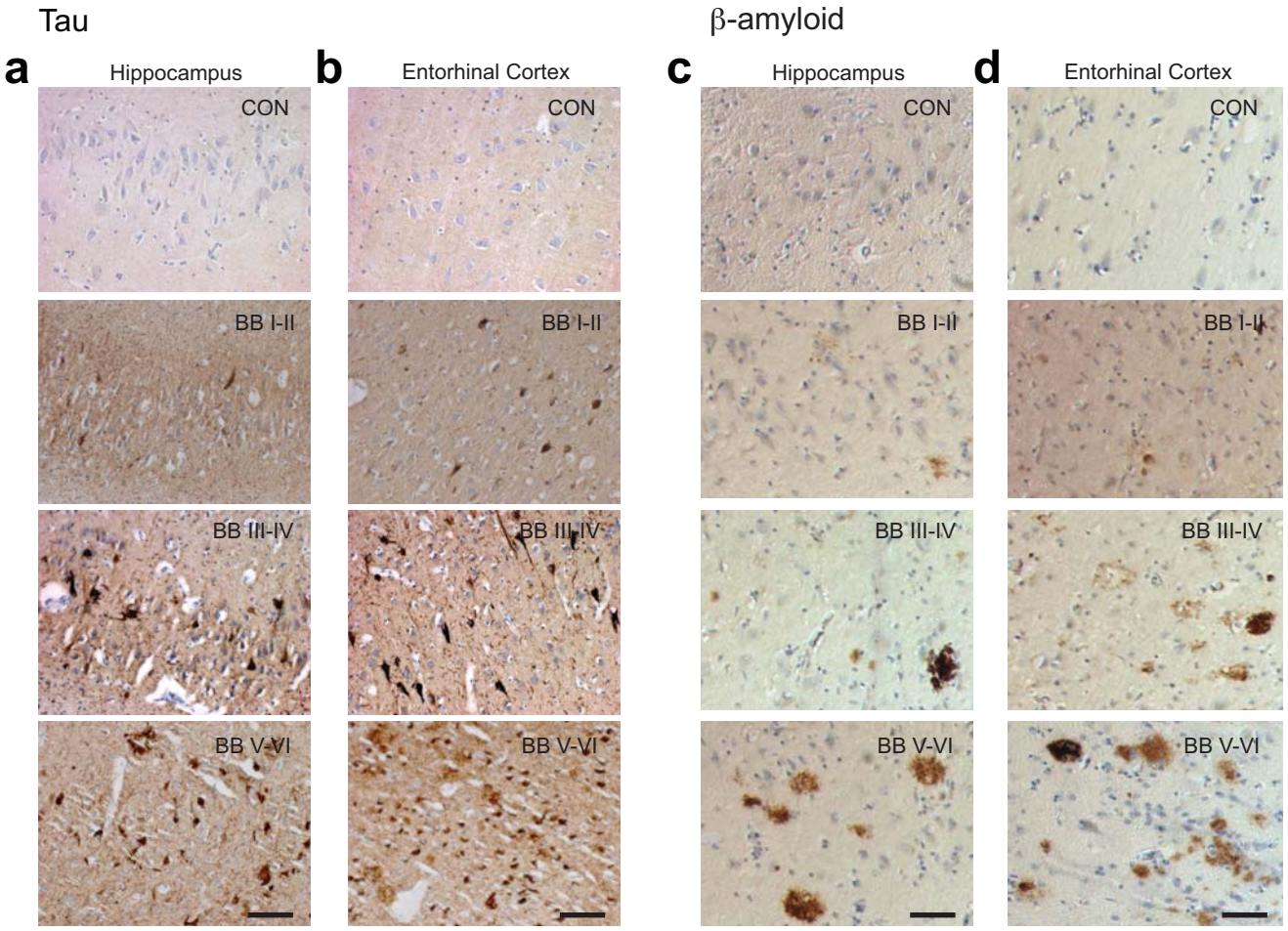

Supplementary Figure 18. Tau tangles and β-amyloid accumulate in the hippocampus and the entorhinal cortex as Alzheimer's disease progresses. a, **b**, Representative images of the cases analyzed in this study showing the accumulation of tau tangles (dark-brown spots) during the development of the Braak and Braak (BB) stages of Alzheimer's disease in (**a**) hippocampal area CA1 and (**b**) the entorhinal cortex. **c**, **d**, Representative images of the cases analyzed in this study showing the accumulation of β-amyloid (dark-brown aggregations) during the development of the Braak and Braak (BB) stages of the disease in (**c**) hippocampal area CA1 and (**d**) the entorhinal cortex; scale bar, 100μm.

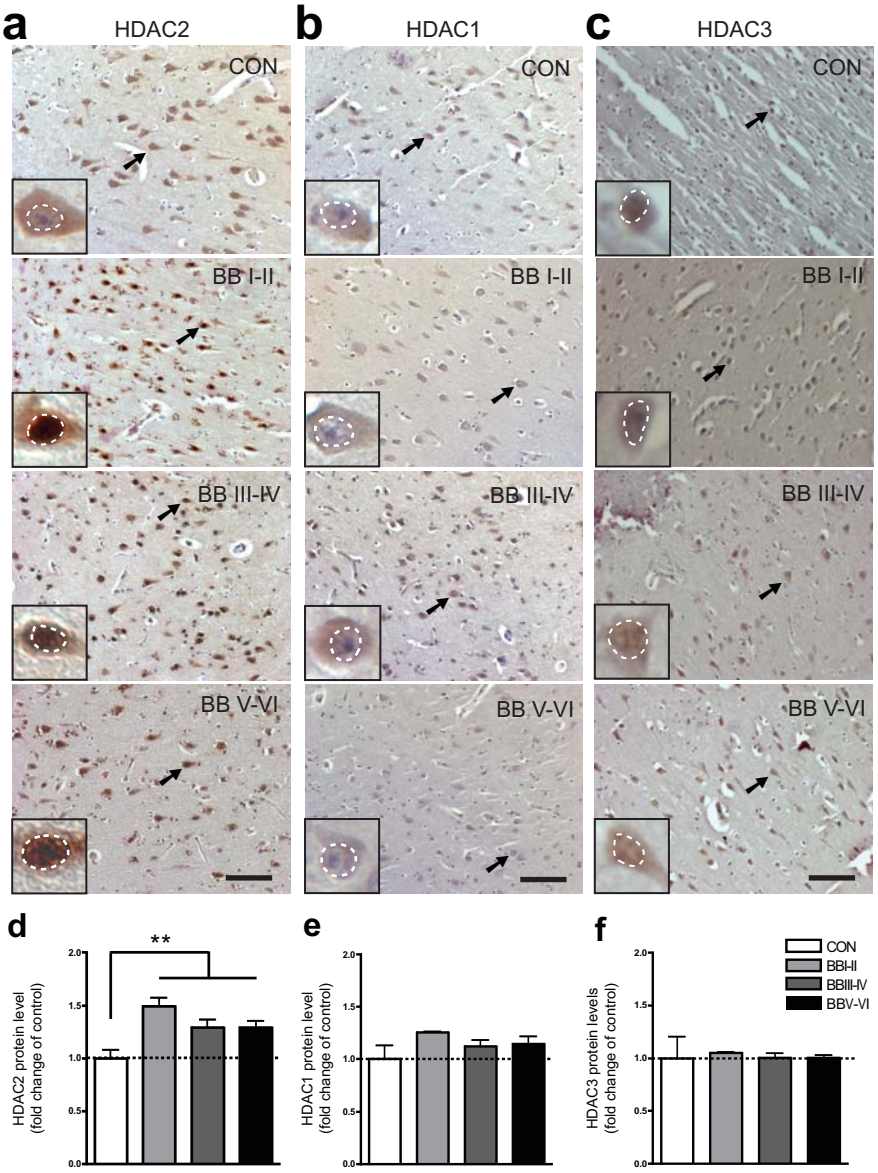

Supplementary Figure 19. HDAC2, but not HDAC1 or HDAC3 levels are increased in the entorhinal cortex during the progression of Alzheimer's disease. a-c, Representative immunohistochemical images depicting (**a**) HDAC2, (**b**) HDAC1, and (**c**) HDAC3 levels in neuronal nuclei in the entorhinal cortex of patients with Braak and Braak (BB) stages I/II (n=4), III/IV (n=7) and V/VI (n=7) compared to BB0 healthy control brains (CON, n=7); insets show magnification of one neuron (indicated by an arrow, nucleus surrounded by white dotted circles); scale bar, 100μm. **d-e**, Quantitative assessment of **a-c**, **p≤0.01; values are mean ± s.e.m.

Supplementary Table 1
Evidence for reduced expression of Alzheimer's disease-related HDAC2 target genes

Gene	Evidence	Sample type	Reference
Arc	mRNA	Human post-mortem AD brain	Ginsberg et al., 2002
		Amyloid-containing post-mortem human brain regions	Dickey et al., 2005
	protein	β-amyloid treated primary cortical neurons	Wang et al., 2005
Bdnf	mRNA	Human post-mortem AD brain	Philips et al., 1991; Murray et al., 1994; Colangelo et al., 2002; Tan et al., 2010
Cdk5	mRNA	Human post-mortem AD brain	Ginsberg et al., 2002; Liang et al., 2008; Tan et al., 2010
Egr1	mRNA	β-amyloid treated human brain pericytes	Rensink et al., 2002/4
		Amyloid-containing post-mortem human brain regions	Dickey et al., 2005
Homer1	mRNA	Amyloid-containing post-mortem human brain regions	Dickey et al., 2005
	protein	β-amyloid treated primary cortical neurons	Roselli et al., 2009
GluR1	mRNA	Human post-mortem AD brain	Ginsberg et al., 2002
	protein	Human post-mortem AD brain	Wakabayashi et al., 1999
GluR2	mRNA	Human post-mortem AD brain	Ginsberg et al., 2002
	mRNA/protein	Galanin-negative neurons in human post-mortem AD brain	Counts et al., 2009; Tan et al., 2010
Nfl	mRNA	Human post-mortem AD brain	McLachlan et al., 1988; Clark et al., 1989; Kittur et al., 1994; Colangelo et al., 2002; Ginsberg et al., 2002
NR2A	mRNA	Human post-mortem AD brain	Ginsberg et al., 2002; Bi and Sze 2002; Tan et al., 2010
NR2B	mRNA	Human post-mortem AD brain	Ginsberg et al., 2002; Bi and Sze 2002
Svp	mRNA	Human post-mortem AD brain	Heffernan et al., 1998; Callahan et al., 1999; Colangelo et al., 2002; Ginsberg et al., 2002; Mufson et al., 2002
Stg	mRNA	Human post-mortem AD brain	Ginsberg et al., 2002; Mufson et al., 2002; Tan et al., 2010

Arc, activity-regulated cytoskeleton-associated protein; Bdnf, brain-derived neurotrophic factor; Cdk5, cyclin-dependent kinase 5; Egr1, early growth response protein 1; GluR, glutamate receptor; Nfl, neurofilamin; NR2, N-methyl D-aspartate receptor subtype 2; Svp, synaptophysin; Stg, synaptotagmin.

Supplementary Table 2
Primer sequences used for promoter amplification

Promoter	Forward (5'-3')	Reverse (5'-3')
Arc	CAGCATAAATAGCCGCTGGT	GAGTGTGGCAGGCTCGTC
Bdnf 1	TGATCATCACTCACGACCACG	CAGCCTCTCTGAGCCAGTTACG
Bdnf 2	TGAGGATAGTGGTGGAGTTG	TAACCTTTTCCTCCTCC
Bdnf 4	GCGCGGAATTCTGATTCTGGTAAT	GAGAGGGCTCCACGCTGCCTTGACG
Cdk5	CGCAGCCTGTTGGACTTTGT	GCGTTGCAGAGGAGGTGGTA
Egr1	GTGCCCACCACTCTTGGAT	CGAATCGGCCTGTATTTCAA
Homer1	CTGCCTGAGTGTCGTGGAAG	ATGATTTCACTCGCGCTGAC
GluR1	GGAGGAGAGCAGAGGGAGAG	TTCCTGCAATTCCTTGCTTG
GluR2	GCGGTGCTAAAATCGAATGC	ACAGAGAGGGGCAGGCAG
Nfl	GCCAGACGAAAGTCAGGAAG	TTTTCACCAGCAGTTTGCAG
NR2A	TCGGCTTGGACTGATACGTG	AGGATAGACTGCCCCTGCAC
NR2B	CCTTAGGAAGGGGACGCTTT	GGCAATTAAGGGTTGGGTTC
Svp	CTAGCCTCCCGAATGGAATG	CAGCAGCAGCATCAGCAATG
Stg	CTGAACAGGTTGAGGGCATT	CCTGAGGAGAGGGGTTTAGG
β-actin	CCCATCGCCAAAACTCTTCA	GGCCACTCGAGCCATAAAAG
β-globin	TGACCAATAGTCTCGGAGTCCTG	AGGCTGAAGGCCTGTCCTTT
β-tubulin	TCCAGGGATGAAGAATGAGG	TGAGCACTGGTAGGGAGCTT
HDAC2		
Segment 1	TCTGGCTAGAAGCACATCCA	TAGGTGTGGGCAAAAGAAGG
Segment 2	CCTTCTTTTGCCCACACCTA	TGGCAGACTCCTTGTATCTCC
Segment 3	CCGAGTCCTGGAAATGCTTA	ACCTGGTGGTCCGATATTCC
Segment 4	ATATCGGACCACCAGGTAGC	TTTAGCCCCTTGCTCAGAGA
Segment 5	TAAGACCGAGGGGTGAACCT	CCAGGGCGACAGTAGTGTTT
Segment 6	CCCGTAGAAACACTACTGTCG	GTAGGGCACAGAGCGGGATA
Segment 7	TATCCCGCTCTGTGCCCTAC	CGCCTCCTTGACTGTACGC
Segment 8	CATGGCGTACAGTCAAGGAG	TCTATGAGGCTTCATGGGATG
Segment 9	TATTATGGCCAGGGTCATCC	GACGTTAAATCTCTGCATCTGCT

Arc, activity-regulated cytoskeleton-associated protein; Bdnf 1, brain-derived neurotrophic factor, promoter region of exon I; Cdk5, cyclin-dependent kinase 5; Egr1, early growth response protein 1; GluR1, glutamate receptor 1; Nfl, neurofilamin; NR2, N-methyl D-aspartate receptor subtype 2; Svp, synaptophysin; Stg, synaptotagmin; HDAC2, histone deacetylase 2; segment 1, first segment amplified in the 1300bp-long HDAC2 promoter region (see Fig. 3l).

Supplementary Table 3
Primer sequences used for coding sequence amplification

Coding region	Forward (5'-3')	Reverse (5'-3')	Amplicon position (bp from TSS)
Arc	GAAGTGGTGGGAGTTCAAGC	CTCCTCAGCGTCCACATACA	753
Bdnf	CATTCAGCACCTTGGACAGA	CAGCCTACACCGCTAGGAAG	707
Cdk5	GGCTAAAAACCGGGAAACTC	CCCAATACCAGCCCAGTCTA	622
Egr1	GGGAGGGTTTGTTTTGATGA	TTTCAACAGCTGACGCAAAC	553
Homer1	CATAGCCAAAAGCCGGTCTA	ATCATTGCCAACCTTGTTCC	645
GluR1	CACATGTAGCCGGAGTGATG	CACTCAAGAGGATGGGGAAA	622
GluR2	ATTTCGGGTAGGGATGGTTC	ACCATCCTTCACTGGCATTC	640
Nfl	GACAGCCTGATGGACGAGAT	GGCTCTTGAACCACTCTTCG	640
NR2A	TGAGAATTGCTCGGTGTCTG	ACCTGGCACTGTAGGAATGG	564
NR2B	GGCTACGGCTACACATGGAT	CCTCTTCTCGTGGGTGTTGT	582
Svp	CTCCTCGGCTGAATTCTTTG	CATTGGCCCTTTGTTGTTCT	306
Stg	CGATGCTGAAACTGGACTGA	GGCAGCAGGAAGACTTTGAC	363
β-actin	TGTTACCAACTGGGACGACA	ACCTGGGTCATCTTTTCACG	312
β-globin	CCTTTTTAGGCTGCTGGTTG	AGAATAGCCAGGGGAAGGAA	200
β-tubulin	GCCAAGTCACAATGGAGGTT	ACAGCTTTCAACAGCCCAGT	745

Arc, activity-regulated cytoskeleton-associated protein; Bdnf, brain-derived neurotrophic factor; bp, base pairs; Cdk5, cyclin-dependent kinase 5; Egr1, early growth response protein 1; GluR1, glutamate receptor 1; Nfl, neurofilamin; NR2, N-methyl D-aspartate receptor subtype 2; Svp, synaptophysin; Stg, synaptotagmin; TSS, transcriptional start site.

Supplementary Table 4
Primer sequences used for exon amplification

Gene	Forward (5'-3')	Reverse (5'-3')
Arc	GTTGACCGAAGTGTCCAAGC	CGTAGCCGTCCAAGTTGTTC
Bdnf exon I	CTCAAAGGGAAACGTGTCTCT	TCACGTGCTCAAAAGTGTCAG
Bdnf exon II	CTAGCCACCGGGGTGGTGTAA	TCACGTGCTCAAAAGTGTCAG
Bdnf exon IV	TGCGAGTATTACCTCCGCCAT	TCACGTGCTCAAAAGTGTCAG
Cdk5	CTCATGAGATTGTGGCTCTG	GACGTGGAGTACAGCTTGGC
Egr1	AGCGAACAACCCTATGAGCA	TCGTTTGGCTGGGATAACTC
GAPDH	AGAGAGGGAGGAGGGGAAATG	AACAGGGAGGAGCAGAGAGCAC
GluR1	GTGGTGGTGGACTGTGAATC	TTGGCGAGGATGTAGTGGTA
GluR2	TGTGTTTGTGAGGACTACGGCA	GGATTCTTTGCCACCTTCATTC
HDAC1	TGCGTGGAAAGAAAACAACC	ACCCAGACCCCTCCTAAATG
HDAC2	GGGACAGGCTTGGTTGTTTC	GAGCATCAGCAATGGCAAGT
HDAC3	GCCAAGACCGTGGCGTATT	GTCCAGCTCCATAGTGGAAGT
Homer1	AGCAGAAGGAAGGCTTGACT	CACGGTACGGCCAATAACTA
Nfl	AGCTGGGTGATGCTTACGAC	AGCTGCACTTGAGCCTTCTC
NR2A	TGCAAGTTACACAGCCAACC	ATCGGAAAGGCGGAGAATAG
NR2B	CCCAGATCCTCGATTTCATT	GCCAAACTGGAAGAACATGG
Svp	GCCACGGACCCAGAGAACAT	GGAAGCCAAACACCACTGAG
Stg	CATCGACCAGATCCACTTGT	TCGTTTCCTACTTGGCACAC
β-actin	GGGAAATCGTGCGTGACATT	CGGATGTCAACGTCACACTT
β-globin	AGCTGCATGTGGATCCTGAGA	GATAGGCAGCCTGCACTGGT
β-tubulin	TAGTGGAGAACACAGACGAGA	CTGCTGTTCTTACTCTGGATG

Arc, activity-regulated cytoskeleton-associated protein; Bdnf I, brain-derived neurotrophic factor exon I; Cdk5, cyclin-dependent kinase 5; Egr1, early growth response protein 1; GAPDH, glyceraldehyde-3-phosphate dehydrogenase; GluR, glutamate receptor; HDAC, histone deacetylase; Nfl, neurofilamin; NR2, N-methyl D-aspartate receptor subtype 2; Svp, synaptophysin, Stg, synaptophysin.

Supplementary Table 5
Case details

Sample ID	Diagnosis	Sex	Age (years)	Postmortem Interval (hours)
BM1	BB0	m	58	19
BM9	BB0	f	72	23
BM11	BB0	f	73	13
BM16	BB0	f	73	26
BM17	BB0	f	77	47
MADRC912	BBIII/IV	f	103	5
MADRC1301	BBI/II	m	85	24
MADRC1314	BB0	m	56	36
MADRC1315	BBV/VI	f	64	9
MADRC1323	BBIII/IV	m	94	24
MADRC1325	BBV/VI	f	80	30
MADRC1360	BBV/VI	f	88	31
MADRC1368	BBIII/IV	f	95	24
MADRC1377	BBV/VI	m	78	24
MADRC1401	BBIII/IV	m	90	24
MADRC1424	BBV/VI	m	89	25
MADRC1433	BBIII/IV	m	87	48
MADRC1434	BBV/VI	f	89	6
MADRC1454	BBI/II	m	85	9
MADRC1476	BBV/VI	f	86	14
MADRC1477	BBI/II	f	92	12
MADRC1483	BBV/VI	f	90	30
MADRC1492	BB0	f	87	4
MADRC1510	BBIII/IV	m	73	22
MADRC1522	BBI/II	f	68	23
MADRC1531	BBIII/IV	f	85	12
MADRC1564	BBV/VI	m	90	12
MADRC1576	BBI/II	m	88	n.d.

BB, Braak and Braak stage; BB0, cases with no neurofibrillary tangles and thus considered healthy controls; BM, Boston Medical Center; MADRC, Massachusetts Alzheimer Disease Research Center at Massachusetts General Hospital; n.d., not defined.